Can stimulated Raman pumping cause large population transfers in isolated molecules?

Nandini Mukherjee and Richard N. Zare[a)]
Department of Chemistry, Stanford University, Stanford, California 94305-5080, USA

(Received 2 September 2011; accepted 13 October 2011; published online 9 November 2011)

When stimulated Raman pumping (SRP) is applied to a stream of isolated molecules, such as found in a supersonic molecular beam expansion, we show that SRP can neither saturate nor power broaden a molecular transition connecting two metastable levels that is resonant with the energy difference between the pump and Stokes laser pulses. Using the optical Bloch-Feynman equations, we discuss the pumping of the hydrogen molecule from H_2 ($v = 0, J = 0, M = 0$) to H_2 ($v = 1, J = 2, M = 0$) as an illustration of how coherent population return severely reduces the SRP pumping efficiency unless the pump and Stokes laser pulses are applied with an appropriate relative delay and ratio of intensities. © *2011 American Institute of Physics*. [doi:10.1063/1.3657832]

I. INTRODUCTION

Stimulated Raman pumping (SRP) is a well-known technique[1–24] for preparing molecules in excited vibrational levels for subsequent experiments. In brief, a pump laser pulse of frequency ω_P and a Stokes laser pulse of frequency ω_S are adjusted so that their frequency difference meets the resonance condition, that is, the energy difference between the two levels 0 and 1, i. e.,

$$\hbar(\omega_P - \omega_S) = E_1 - E_0. \tag{1}$$

By irradiating a molecular sample with the two pulses, molecules are transferred from level 0 to level 1. It is commonly accepted wisdom that in a high-pressure environment where the rate of collisions is comparable to or larger than the pumping rate, SRP can achieve population transfer with an efficiency that approaches 50% at saturation. Therefore, it is easy to imagine that the same efficiency might apply to isolated molecules. However, experiments done by others[21] and by us[24] indicate a much poorer performance, which is not improved by simply increasing the powers of the pump and Stokes pulses. We revisit the stimulated Raman pumping of an isolated molecule using intense nanosecond laser pulses and show that in the absence of dephasing, population transfer to an excited vibrational state can be severely limited by coherent population return (CPR).[25,26] CPR occurs during pulsed excitation when the resonance condition is not satisfied. The resonance condition is defined through a detuning δ as follows:

$$\delta = \omega_P - \omega_S - (E_1 - E_0)/\hbar < 1/\tau, \tag{2}$$

where $1/\tau$ is the inverse pulse duration or inverse interaction time between the optical fields and the molecule.

At the laser intensity of tens of GW/cm^2 typically used for SRP, ac Stark shifts of the vibrational levels, which are on the order of several GHz,[14] dynamically destroy the Raman resonance condition, defined by Eqs. (1) and (2). But, under the condition of coherent excitation, the stimulated absorption spectra of isolated molecules are free from power and Stark broadening. As explained later, the linewidth of the SRP transition is only a fraction of a GHz, which arises from the inverse interaction time for optical pulses of a few nanoseconds.

We utilize the Bloch vector model of Feynman, Hellwarth, and Vernon[27] to explain how CPR makes the population transfer to be extremely sensitive to the laser power and frequency detuning when the system is adiabatically excited using nanosecond laser pulses. Although CPR (Refs. 25 and 26) has been discussed previously in the context of coherently driven two-level atomic systems, it has not been given proper attention in discussing stimulated Raman pumping for preparing isolated, vibrationally excited molecular targets. As a practical and useful example, we numerically analyze the S(0) branch of SRP for the hydrogen molecule, which causes the transition H_2 ($v = 0, J = 0, M = 0$) to H_2 ($v = 1, J = 2, M = 0$). We calculate the vibrational excitation using commercially available green (second harmonic of Nd:$^{+3}$YAG at 532 nm) and red (699 nm dye-laser) nanosecond laser pulses with energies in the range of 10–100 mJ.

We construct the Bloch-Feynman vector model from the density matrix equations describing the stimulated Raman pumping. The vector model provides an intuitive picture for the adiabatic passage and coherent population return. A quantitative picture is provided through the numerical results of pumping the H_2 molecule in the presence of dynamic Stark shifts. To show explicitly how the Raman spectrum narrows in a collision-free environment, we calculate the spectrum of coherent versus incoherent Raman pumping. Finally, we discuss how CPR can be circumvented and complete population of the ground vibrational level can be transferred to a desired excited vibrational level using Stark-induced adiabatic Raman passage (SARP) with partially overlapping pump and Stokes pulses of appropriate intensities. In the following discussion we assume Doppler-free excitation which is certainly

[a)]Author to whom correspondence should be addressed. Electronic mail: zare@stanford.edu.

a valid assumption for a reasonably collimated molecular beam. Note that Raman excitation in a gas cell can be made significantly Doppler-free at reduced temperature using co-propagating pump and Stokes laser beams.

II. BLOCH-FEYNMAN VECTOR MODEL FOR SRP

In the absence of an intermediate level that lies close to the frequencies of the pump and Stokes laser pulses, the SRP process is conveniently described by the following density matrix equations involving the two resonant vibrational (initial $v = 0$ and final $v = 1$) levels:

$$\frac{d\sigma_{01}}{dt} + i\delta_2\sigma_{01} = i2rw, \tag{3}$$

and

$$\frac{dw}{dt} = -2\mathrm{Im}[r^*\sigma_{01}]. \tag{4}$$

The derivation of Eqs. (3) and (4) have been presented in Refs. 28 and 29 and can also be derived starting from the treatment presented by Chelkowski and Bandrauk.[30] Here, σ_{01} is the slowly varying amplitude of the off-diagonal element of the 2×2 density matrix $\boldsymbol{\rho}$ representing the two-photon resonant rovibrational system. Specifically, σ_{01} is a measure of the two-photon Raman coherence between the $v = 0$ and $v = 1$ vibrational levels. The quantity $w = (\rho_{11}-\rho_{00})/2$ measures the population inversion, where ρ_{11} and ρ_{00} are the fractional populations in the $v = 1$ and $v = 0$ levels, respectively. The quantity r is the generalized two-photon Rabi frequency given by

$$r = \frac{E_P E_S^*}{\hbar^2}\sum_k \mu_{0k}\mu_{k1}\left[\frac{1}{(\omega_{k0}-\omega_P)} + \frac{1}{(\omega_{k0}+\omega_S)}\right], \tag{5}$$

where E_P and E_S are the slowly varying electric field amplitudes of the laser pulses with pump frequency ω_P and Stokes frequency ω_S. The quantities μ_{ik} and $\omega_{ki} = \omega_{v'v}$ are the transition dipole moments and the resonance frequency associated with the $i \rightarrow k$ vibronic transitions between the ground and excited electronic manifold. The net time-dependent detuning δ_2 for the $v = 0 \rightarrow v = 1$ Raman transition is given by

$$\delta_2 = \delta_0 - \delta_{\mathrm{ac}} - i\gamma, \tag{6}$$

where γ is the phenomenological dephasing rate for the Raman coherence σ_{01} caused by collisions or by phase fluctuations of the optical fields. Here, $\delta_0 = \omega_P$-ω_S-ω_{10} is the zero-field or static detuning of the $0 \rightarrow 1$Raman transition, and δ_{ac} is the time-dependent dynamic Stark shift of the Raman resonance in the presence of pump and Stokes laser pulses. For the visible pump and Stokes waves with far off-resonant excited electronic states as in the H_2 molecule, the net Stark shift δ_{ac} depends upon the difference between the dispersionless, i.e., $\alpha_i(\omega_P) \cong \alpha_i(\omega_S)$, polarizabilities of the ground and excited vibrational levels as expressed by the following equation:[29]

$$\delta_{\mathrm{ac}} \cong -\frac{(\alpha_1 - \alpha_0)}{\hbar}[|E_P|^2 + |E_S|^2]. \tag{7}$$

We need to stress that the molecular polarizabilities are orientation-dependent.[14] Thus, for a diatomic molecule, there is a difference between the polarizability along the internuclear axis and that perpendicular to the internuclear axis. Using the S(0) branch of Raman transition in the following we show that even for the least polarizable H_2 molecule appreciable ac Stark shift at a pump intensity of few tens of GW/cm^2 influences the dynamics of population transfer.

In the absence of phase damping characterized by $\gamma = 0$, Eqs. (3) and (4) can be transformed into a single equation that describes a rotating pseudo-vector (often called the two-photon Bloch vector) $\boldsymbol{R}$ around an angular velocity vector $\boldsymbol{F}$ (also referred to as the field vector) in a three-dimensional abstract space:[27,31–35]

$$\frac{\mathrm{d}\boldsymbol{R}}{\mathrm{dt}} = \boldsymbol{F} \times \boldsymbol{R}, \tag{8}$$

where $\boldsymbol{F} = \{-2\mathrm{r},\ 0,\ -\delta_2\}$ and $\boldsymbol{R} = \{\mathrm{Re}(\sigma_{01}),\ \mathrm{Im}(\sigma_{01}),\ w\}$. The components of $\boldsymbol{F}$ contain the properties of the laser fields that can be manipulated, and the components of $\boldsymbol{R}$ contain the properties of the two-level molecular system that evolve under the action of $\boldsymbol{F}$. Using this Bloch vector model, we can draw a simple intuitive picture of stimulated Raman pumping as follows. At the starting point of the Raman interaction, we have $r \approx 0$, $\sigma_{01} \approx 0$, and $w \approx -0.5$. At this initial time if the static detuning $\delta_0 \neq 0$, both $\boldsymbol{F}$ and $\boldsymbol{R}$ point parallel to the z axis of the abstract space. As the two-photon Rabi frequency r develops and the Raman detuning δ_2 is Stark-shifted under the action of the pump and Stokes laser pulses, $\boldsymbol{F}$ starts changing direction in the xz plane of the abstract space. If $\boldsymbol{F}$ changes sufficiently slowly compared to the angular velocity $|\boldsymbol{F}|$ then $\boldsymbol{R}$ follows the instantaneous position of $\boldsymbol{F}$ rotating about it. This behavior is called adiabatic following. As a consequence of adiabatic following, $\boldsymbol{R}$ traces a narrow conical surface around $\boldsymbol{F}$, all the time staying nearly parallel to $\boldsymbol{F}$. The adiabatic following condition can be expressed mathematically as[29,33]

$$\frac{|\Delta\boldsymbol{F}|}{|\boldsymbol{F}|} \sim \frac{|\mathrm{d}\boldsymbol{F}/\mathrm{dt}|}{|\boldsymbol{F}|^2} < 1. \tag{9}$$

The adiabatic condition is well satisfied with the nanosecond pump and Stokes laser pulses with energies of few tens of mJ. Partial population transfer occurs when w changes as the Bloch vector $\boldsymbol{R}$ is dragged along by the relatively slowly rotating field vector $\boldsymbol{F}$ in the xz plane. At the end of the pulsed excitation as $r \rightarrow 0$ and $\delta_2 \rightarrow \delta_0$, both $\boldsymbol{F}$ and $\boldsymbol{R}$ return to their initial (beginning of interaction) positions. Thus, population transferred to the excited state during the peak of the interaction is coherently driven back to the ground state at the end of excitation. This cycling of population is known as CPR. It is important to note the basic difference between the adiabatic passage and the Rabi oscillations of the Bloch vector. Rabi oscillations occur near a static detuning $\delta_0 \approx 0$, when $\boldsymbol{F}$ moves along a straight line instead of rotating in the xz plane. It is easy to see that with the zero static detuning the ratio F_z/F_x stays constant while the Stark shifted detuning δ_2 and the Raman coupling r change in phase under the action of the laser pulses. In this case, the Bloch vector $\boldsymbol{R}$ rotates on the surface of a cone about the fixed direction of $\boldsymbol{F}$ leading to the Rabi oscillations of population as a function of laser fluence.

III. RESULTS OF NUMERICAL SIMULATIONS

Equations (3) and (4) were numerically integrated assuming Gaussian temporal profiles for the pump and Stokes laser pulses with 1/*e* half widths of 6 ns. The pump and Stokes laser pulses are applied with a zero delay between them. The time-dependent ac Stark shifts of the rovibrational levels H_2 ($v = 0$, $J = 0$, $M = 0$) and H_2 ($v = 1$, $J = 2$, $M = 0$) and the Raman coupling r are calculated using the time-dependent intensity of the laser pulses at each step of the numerical integration. The molecular parameters are taken from Ref. 29. To simulate a most common example of SRP, these calculations assume a stronger pump pulse at 532 nm (frequency-doubled Nd^{+3}:YAG laser), and a relatively weaker Stokes pulse at 699 nm (amplified pulsed dye laser). The results are not affected by using pump and Stokes laser pulses of equal amplitudes.

The temporal dynamics of stimulated Raman pumping for three different static detunings are presented for $\delta_0 = 0.0$ GHz in Fig. 1, for $\delta_0 = 0.5$ GHz in Fig. 2, and for $\delta_0 = -0.6$ GHz in Fig. 3. With the static detuning of $\delta_0 = 0.0$ GHz, Fig. 1(a) shows that ac Stark shift modifies the net

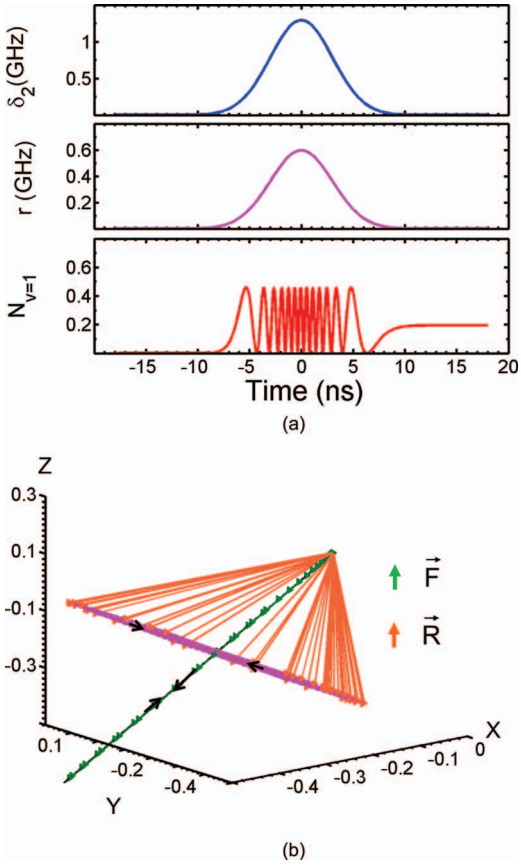

FIG. 1. Rabi Oscillations in stimulated Raman pumping of H_2 ($v = 0$, $J = 0$, $M = 0$) $\rightarrow$ H_2 ($v = 1$, $J = 2$, $M = 0$) using Gaussian pump and Stokes optical fields with 1/e widths of $\tau = 6$ ns, a pump fluence = 1 J/mm^2; a Stokes fluence = 0.26 J/mm^2, and static detuning $\delta_0 = 0.0$ GHz. Pump and Stokes pulses are applied with zero relative delay between them. (a) Raman detuning δ_2 (blue), two-photon Rabi frequency r (magenta), and Rabi oscillations of excited state population $N_{v=1}$ (red) as functions of time. (b) Snapshots of the spinning Bloch vector ***R*** (orange) around the fixed direction of the pseudo-angular velocity vector ***F*** (green).

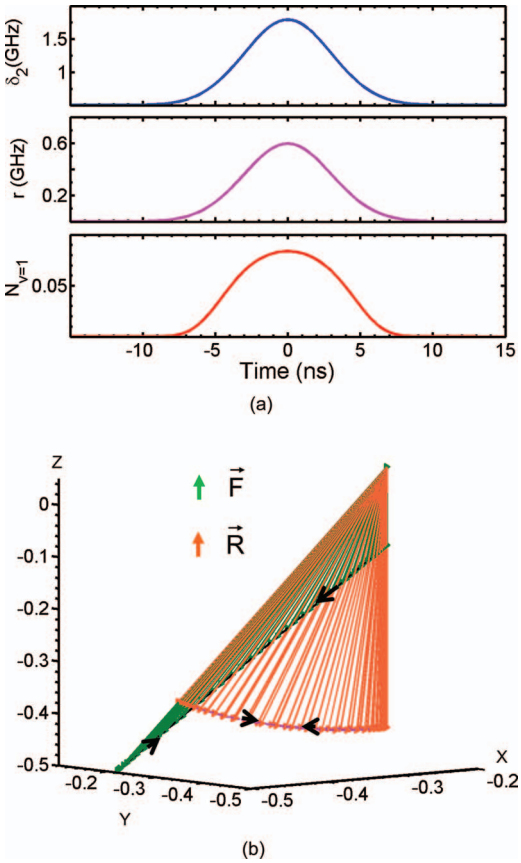

FIG. 2. Coherent population return in stimulated Raman pumping of H_2 ($v = 0$, $J = 0$, $M = 0$) $\rightarrow$ H_2 ($v = 1$, $J = 2$, $M = 0$) for a static detuning $\delta_0 = 0.5$ GHz. The rest of the pulse parameters are identical to that of Fig. 1. (a) Raman detuning δ_2 (blue), two-photon Rabi frequency r (magenta), and fractional population transferred to excited state $N_{v=1}$ (red) as functions of time. (b) Snapshots of adiabatically rotating Bloch vector ***R*** (orange) around the pseudo angular velocity vector ***F*** (green). At the end of excitation, both vectors return to their initial positions.

detuning δ_2 (blue, uppermost panel of Fig. 1(a)) which grows positive with the pulse intensity. Consequently, the molecular system moves far off resonance at the peak of the Raman coupling r (magenta, middle panel of Fig. 1(a)). Because r and δ_2 stay in phase, being proportional to each other, the field vector ***F*** moves along a straight line (green, Fig. 1(b)) in the negative quadrant of the xz plane without changing its direction. As a result, the Bloch vector ***R*** (orange, Fig. 1(b)) spins around the fixed direction of ***F*** generating the Rabi oscillation of population transfer shown by the values of $N_{v=1}$ (red, lowest panel of Fig. 1(a)). It might be thought that appreciable population would be transferred to the excited state by adjusting the pulse fluence or the Raman coupling r; in reality, however, in the presence of finite energy and frequency fluctuations of the pump and Stokes laser pulses it becomes practically impossible to precisely tune to the ideal pulse parameters to achieve appreciable vibrational excitation. Thus, resonant tuning with zero time delay between the pump and Stokes pulses is ineffective in causing population transfer by SRP.

Figure 2 describes the adiabatic passage of stimulated Raman pumping for a positive static detuning of $\delta_0 = 0.5$ GHz. As shown in the upper two panels of Fig. 2(a), δ_2

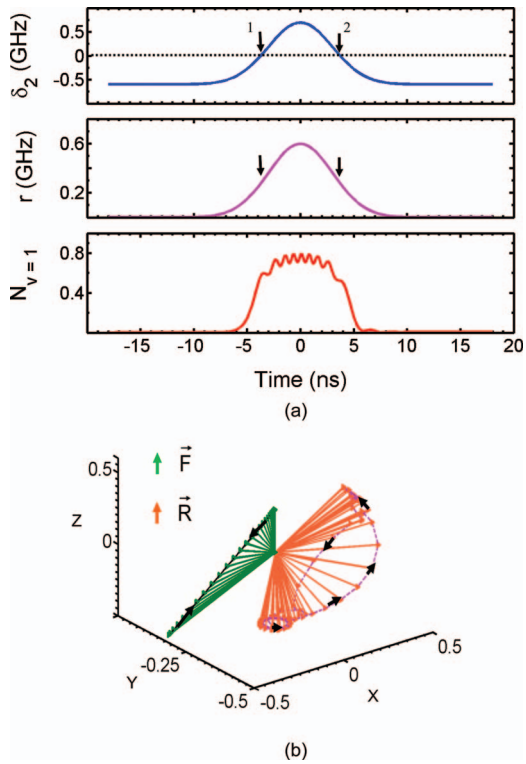

FIG. 3. Transient population inversion during CPR in stimulated Raman pumping of H_2 ($v = 0, J = 0, M = 0$) → H_2 ($v = 1, J = 2, M = 0$) with $\delta_0 = -0.6$ GHz. The pulse parameters are identical to those in Fig. 1. (a) Raman detuning δ_2 (blue), two-photon Rabi frequency r (magenta), and excited state population $N_{v=1}$ (red) as functions of time. (b) Snapshots of adiabatically rotating Bloch vector $\boldsymbol{R}$ (orange) around the pseudo-angular velocity vector $\boldsymbol{F}$ (green). During the pulsed excitation, both $\boldsymbol{R}$ and $\boldsymbol{F}$ flip across the $z = 0$ xy plane twice as the detuning δ_2 sweeps back and forth across the zero value. At the end of excitation $\boldsymbol{R}$ and $\boldsymbol{F}$ return to their initial positions leaving no population in the excited state.

(blue) and r (magenta) grow with increasing intensity of the laser pulses, but they are no longer proportional to each other. This means that the ratio F_z/F_x is changing in time, causing a rotation of the field vector $\boldsymbol{F}$ (green, Fig. 2(b)) in the xz plane. With an appreciable Raman coupling r, the Bloch vector $\boldsymbol{R}$ (orange, Fig. 2(b)) is dragged adiabatically by the field vector $\boldsymbol{F}$. As $\boldsymbol{R}$ tilts in the xz plane modifying w, a small population is transiently excited during the peak of the Raman pumping r, as shown in the lower panels of Fig. 2(a). However, at the end of the excitation, both $\boldsymbol{F}$ and $\boldsymbol{R}$ again return to their original positions leaving no population in the excited state as can be seen from the temporal dynamics of the excited state population $N_{v=1}$ (red, lowest panel, Fig. 2(a)). Because δ_2 does not change sign, $\boldsymbol{F}$ and $\boldsymbol{R}$ stay confined below the $z = 0$ xy plane. In the absence of sign reversal for w, no population inversion occurs during the peak of interaction.

Figure 3 shows another example of coherent population return in which a negative static detuning of $\delta_0 = -0.6$ GHz is partially compensated by the ac Stark shift and the system is dynamically brought into resonance near the peak of the pulses. In this example the adiabatic inversion of the Bloch vector occurs twice during the optical interaction with the pump and Stokes laser pulses. The first time the detuning δ_2 (blue, upper most panel of Fig. 3(a)) sweeps through zero from a negative to a positive value with the rising intensity of the pump and Stokes pulses (shown by arrow 1), it causes $\boldsymbol{F}$ to rotate across $z = 0$ in the xz plane. In the presence of a Raman coupling r, the Bloch vector $\boldsymbol{R}$ is dragged along by the field vector $\boldsymbol{F}$ and reverses direction along the z-axis, which implies a sign change in w. Reversal of w means population inversion. During the second excursion, δ_2 crosses zero approaching from a positive toward a negative value as shown by arrow 2 in the top panel of Fig. 3(a), again causing both $\boldsymbol{F}$ and $\boldsymbol{R}$ to flip along the z-axis of the abstract space, bringing the excited population back to the ground state as shown clearly in the lowest panel of Fig. 3(a). The adiabatic following of the Bloch vector $\boldsymbol{R}$ around the field vector $\boldsymbol{F}$ is depicted in Fig. 3(b). This is an example showing how the ac Stark sweeping of the Raman resonance causes CPR which goes through a population inversion.

In all three cases considered (Figs. 1–3), SRP with zero time delay between the pump and Stokes pulses is rather ineffective in bringing about population transfer irrespective of the exact frequency match or mismatch with the vibronic energy level difference. Increasing the intensity of the pump and the Stokes pulses does not improve this dismal outcome.

To provide more perspective on this problem we calculated the Raman population transfer for a wide range of pulse fluence and static detuning δ_0 as shown in the three-dimensional plot of Fig. 4(a). Figure 4(b) shows a contour map for the range of pump fluence and detuning δ_0 that achieves more than 50% population transfer. The absence of power broadening is clearly seen in this figure. Figures 4(a) and 4(b) should be convincing how difficult it would be in practice to meet the restricted set of pulse parameters to achieve a significant vibrational excitation without sophisticated frequency and energy stabilizations.

In Fig. 5, we show the population in the stimulated Raman pumped level $v = 1$ versus laser frequency and fluence for coherent compared to incoherent pumping conditions. Figure 5(a) shows the population transferred to $v = 1$ level as a function of pump fluence for two different zero-field detunings $\delta_0 = 0$ GHz and $\delta_0 = -0.5$ GHz for the cases of coherent (upper panel, $\gamma = 0$ GHz) and incoherent (lower panel, $\gamma = 1.0$ GHz) excitations. The incoherent case corresponds either to a gas cell with a pressure of a few Torr or a broadband pump radiation with a phase fluctuation rate of $\gamma = 1.0$ GHz. Figure 5(a) shows that in the coherent case, the population transfer oscillates as a function of pulse fluence and the amplitude depends sensitively on the zero-field detuning. For the case of incoherent excitation (lower panel, Fig. 5(a)), the population transfer shows saturation as a function of laser fluence. The saturation threshold hardly depends on the small zero-field frequency detuning of −0.5 GHz. Figure 5(b) compares the coherent (upper panel, $\gamma = 0$ GHz) excitation spectrum with that of an incoherent case (lower panel, $\gamma = 1.0$ GHz) for two different pump fluences of 1 and 2 J/mm^2 (corresponding peak intensities of ∼15 and 30 GW/cm^2 for ∼7 ns pulses). The absence of power broadening for the coherent Raman pumping is clearly shown by the narrow spectrum of ∼0.4 GHz for both fluences. This spectral width matches the linewidth of the pump and Stokes pulses. Contrary to

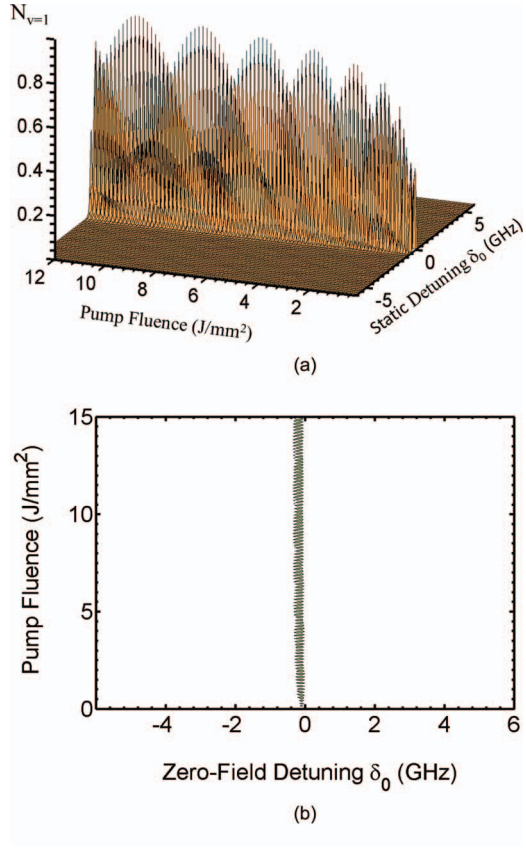

FIG. 4. Coherent stimulated Raman pumping of H_2 ($v = 0, J = 0, M = 0$) $\rightarrow$ H_2 ($v = 1, J = 2, M = 0$) as functions of pump fluence and static detuning δ_0 (GHz). The pulse duration for the Gaussian pump and Stokes pulses are identical to the previous figures and the pulses are applied with zero delay between them. (a) Three-dimensional plot of the excited state population $N_{v=1}$ as a function of pump fluence (J/mm^2) and static detuning δ_0 (GHz). Note that Rabi oscillation peak height which appears to exceed the value 1 as seen in this plot is not real, but generated artificially by the perspective of this three-dimensional figure. (b) Contour map showing the range of pulse fluence and detuning to achieve more than 50% population transfer.

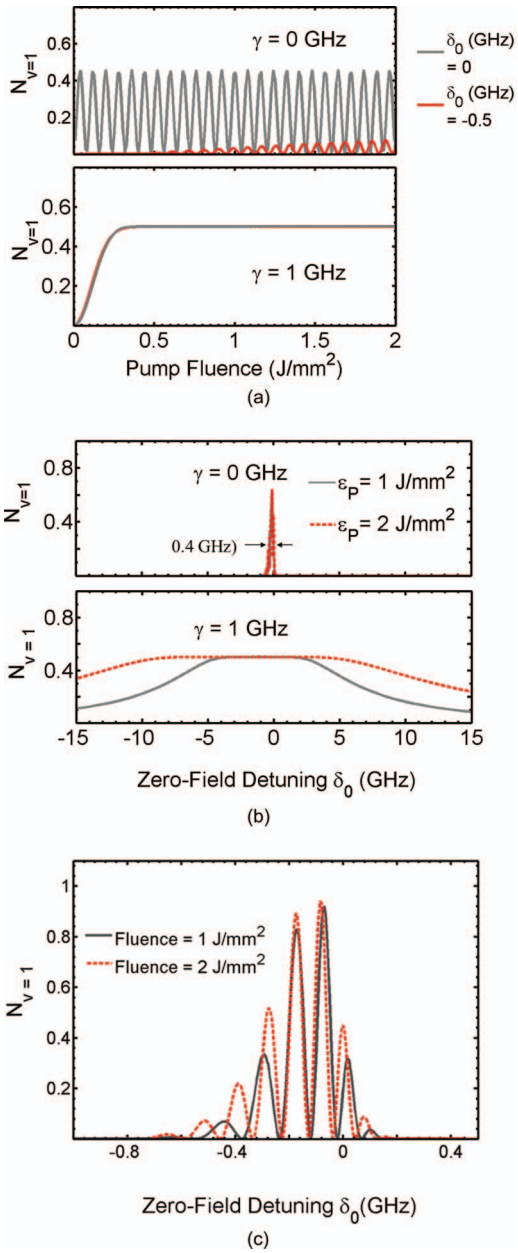

FIG. 5. Coherent versus incoherent stimulated Raman pumping of H_2 ($v = 0, J = 0, M = 0$) $\rightarrow$ H_2 ($v = 1, J = 2, M = 0$). The Gaussian pulse durations and delays are identical to that of the previous figures. (a) Comparison of the fractional excited state population versus pump fluence for two different detunings $\delta_0 = 0$ GHz (gray) and $\delta_0 = -0.5$ GHz (red) for the case of coherent ($\gamma = 0$ GHz, upper panel) and incoherent (($\gamma = 1$ GHz, lower panel) pumping. (b) Excited state fractional population versus static detuning for coherent ($\gamma = 0$ GHz, upper panel) and incoherent ($\gamma = 1$ GHz, lower panel) pumping with two different pump fluences 1 J/mm^2 (gray) and 2 J/mm^2 (red dashed). The narrow spectrum of ~0.4 GHz for the coherent case (upper panel) shows no power broadening. (c) High-resolution spectrum for the coherent case (upper panel of Fig. 5(b)) shows Rabi oscillations for pump fluences of 1 J/mm^2 (gray) and 2 J/mm^2 (red dashed).

what might be expected,[21] at these intensity levels the time-dependent Stark shift $\delta_2 > 2$ GHz does not broaden the stimulated Raman spectrum for the coherent excitation shown in the upper panel of Fig. 5(b). The incoherent excitation at two different pump fluences shows considerable power broadening of Raman pumping (lower panel of Fig. 5(b)) usually observed in a room-temperature gas cell. Figure 5(c) shows a high-resolution picture of the population transfer versus the zero-field detuning corresponding to the coherent spectrum in the upper panel of Fig. 5(b). Rabi oscillations are seen within a spectral bandwidth that increases slightly with the pump fluence. Because we have used a higher frequency resolution in presenting Fig. 5(c) than in Fig. 5(b), the Rabi oscillation peak height in Fig. 5(c) reaches a higher value than the peak excitation seen in Fig. 5(b). Figures 5(a)–5(c) reconfirm that in a collision-free molecular beam the stimulated Raman pumping with intense nanosecond laser pulses can neither be saturated nor power broadened.

IV. DISCUSSION

We have shown that for an isolated molecule coherent population return significantly diminishes the population transfer in stimulated Raman pumping when the pump and Stokes pulses simultaneously arrive at the molecule. This fact has serious consequences in attempting to prepare large

concentrations of vibrationally excited molecules in a molecular beam by direct application of SRP. Vibrational levels of the electronic ground state have radiative lifetimes on the order of milliseconds or longer and consequently, in a collision-free environment effectively no relaxation occurs during the pumping process that employs nanosecond laser pulses. SRP carried out in this manner presents an ideal case for coherent population return, which also applies to the infrared pumping of a dipole-allowed transition. Confirmation of this behavior is provided by the infrared pumping of the HF dimer carried out by Pine and Fraser.[36] They studied the linewidth of two H–F vibrations, one on the outside of the HFHF dimer, the other on the inside. They find that the short-lived inside one, which is associated with the predissociation of the dimer, is significantly more power-broadened compared to the long-lived outside one.

Isolated molecules are quite resistant to pumping by Raman or infrared pulses, and this means that in the absence of resonance, defined by Eq. (2), they can be transiently excited but at the end of the pulse, they almost completely return to the initial level from which they were pumped. This situation is portrayed in Figs. 2–4. This situation must be contrasted with the case of saturation (Fig. 5) in which a maximum of 50% transfer can be reached in the presence of collisions that provide rapid dephasing of the optically induced coherence.

The idea of coherent excitation presented in this paper can be used to explain the small (0.1%) population transfer to $v = 1$ level of CH_4 and H_2 in a supersonic beam using stimulated Raman pumping.[21,24] It is relevant to point out that a grating-tuned pulsed dye laser pumped by an injection-seeded Nd^{+3}:YAG laser dominantly shows single-mode character in a single shot.[37,38] Hence, molecules in a supersonic beam are excited coherently, where CPR as opposed to saturation controls the outcome.

This situation may seem at first to be very disappointing from the viewpoint of preparing large concentrations of vibrationally excited molecules in a single quantum state by irradiating a stream of isolated molecules. However, as we have pointed out previously,[29] it is possible to achieve close to 100% population transfer by means of SARP with nanosecond pump and Stokes pulses. This concept is illustrated in Fig. 6. The pump and Stokes pulses having unequal intensities partially overlap in time so that the Stark shift of the Raman resonance is swept by the stronger pulse to cause an inversion of the Bloch vector $\boldsymbol{R}$. To prevent coherent population return, the delay and the relative intensities of the pulses are adjusted so that the inversion of $\boldsymbol{R}$ occurs only once during the second zero crossing of the Stark shifted detuning δ_2 near the peak of Raman interaction (shown by arrow number 2 in Fig. 6).

Figure 7 shows that using higher fluence it is possible to achieve relative immunity to the moderate fluctuations of laser frequency and fluence and thereby still achieve nearly complete population transfer. This fact makes SARP a robust technique that can be accomplished using pulsed dye lasers without sophisticated frequency and energy stabilization. Figure 8 compares the frequency response of the population transferred to $v = 1$ level for zero delay versus a delay $\tau_D = 1.4\ \tau_P$ appropriate for SARP with Gaussian pump pulses with the $1/e$ half-width of τ_P. For zero-delay the spectrum

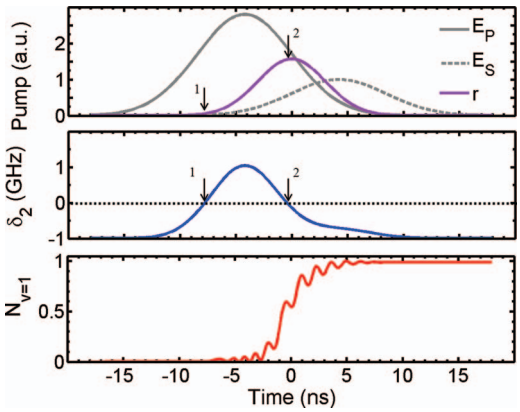

FIG. 6. Complete population inversion of H_2 ($v = 0$, $J = 0$, $M = 0$) $\rightarrow$ H_2 ($v = 1$, $J = 2$, $M = 0$) using SARP with temporally shifted but overlapping Gaussian pump and Stokes pulses. The Gaussian optical fields have $1/e$ widths of $\tau = 6$ ns, a pump fluence $= 2$ J/ mm^2, a Stokes fluence $= 0.26$ J/mm^2, and static detuning $\delta_0 = -1$ GHz. Pump and Stokes pulses are applied with a relative delay $= 1.4\tau$ between them. Uppermost panel shows the pump (solid gray) and Stokes (dashed gray) optical fields as well as the Raman coupling r (purple) in arbitrary units. The middle panel shows sweeping of the Raman detuning δ_2 (blue) by the optical pulses. The lower panel shows the fractional population transfer $N_{v=1}$ (red). The dynamic detuning δ_2 crosses zero two times indicated by arrows. During the first crossing, the Raman coupling r is small as shown by arrow 1 in the upper panel. Population is inverted during the second crossing of zero, shown by arrow 2 in the upper and middle panels.

shows fast Rabi oscillations in frequency which might explain the small population transfer often observed with pulsed lasers whose frequency has not been stabilized. For the same pump fluence the SARP spectrum attains nearly complete population transfer over a broad range of static detuning ~6.5 GHz. In essence, SARP causes a different sort of power broadening, which may be called "coherent power broadening."

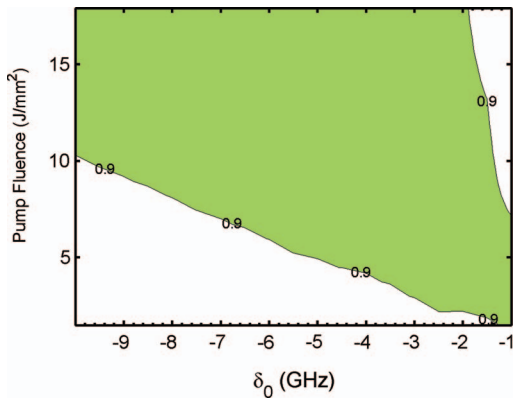

FIG. 7. Contour map for achieving >90% population inversion for the H_2 ($v = 0, J = 0, M = 0$) $\rightarrow$ H_2 ($v = 1, J = 2, M = 0$) transition using SARP with temporally shifted but overlapping Gaussian pump and Stokes pulses versus pulse fluence in (J/mm^2) and static detuning δ_0 in GHz. Gaussian optical fields have $1/e$ widths of $\tau_P = 6$ ns for the pump and $\tau_S = 5$ ns for the Stokes. The optical field amplitude ratio $E_P/E_S = 2.6$. The delay between the pump and Stokes pulses is $1.4\ \tau_P$. The green area represents the range of pump pulse fluence and the static detuning necessary to achieve >90% population transfer. With large enough fluence it is possible to reduce significantly the effects of moderate fluctuation of frequency and energy and achieve nearly complete population transfer to the $v = 1$ excited level.

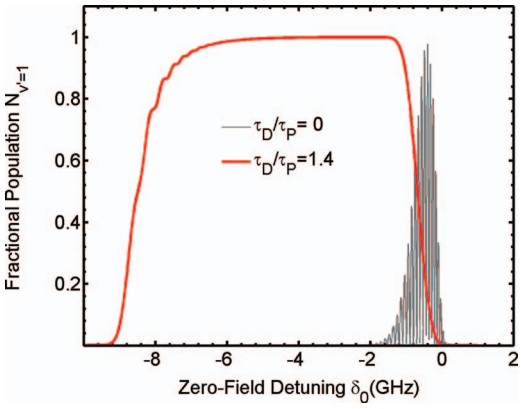

FIG. 8. Population transfer in stimulated Raman pumping of H_2 ($v = 0$, $J = 0$, $M = 0$) → H_2 ($v = 1$, $J = 2$, $M = 0$) versus the static detuning δ_0 in GHz using pump and Stokes Gaussian-shaped laser pulses with zero-delay (gray) and with a delay $\tau_D/\tau_P = 1.4$ (red) appropriate for SARP. Gaussian optical fields have $1/e$ widths of $\tau_P = 6$ ns for the pump and $\tau_S = 5$ ns for the Stokes. The fluences are 7.4 J/mm^2 for the pump pulse, and 1 J/mm^2 for the Stokes pulse. With large enough fluence SARP shows a wider bandwidth for achieving nearly complete population transfer to the $v = 1$ excited level. The zero-delay shows fast Rabi oscillations which makes it an impractical way to achieve substantial population transfer.

In a like manner, coherent population return in infrared pumping of a molecular beam can be circumvented by either chirping the laser frequency or by chirping the vibrational transition frequency. The later may be accomplished by using an additional off-resonant Stark pulse that sweeps the detuning of the vibrational resonance through zero during the interaction with a relatively weak resonant infrared pump pulse. This approach is similar to what Bergmann and co-workers[39–41] introduced for Stark chirped rapid adiabatic passage known as SCRAP, which accomplishes population transfer between two metastable vibrational levels via an intermediate level within the excited electronic manifold. For many molecules therefore, SCRAP requires tunable UV or VUV pulses, making it technically difficult to achieve in practice. However, the exclusive use of vibrational levels of the electronic ground state with their much longer radiative lifetimes allows us to use visible or infrared laser sources, and therefore makes it much easier to accomplish population inversion.

ACKNOWLEDGMENTS

We thank the (U.S.) Army Research Office (USARO) under ARO Grant No. W911NF-10-1-01318 for support of this work.

[1]E. E. Hagenlocker and W. G. Rado, Appl. Phys. Lett. **7**, 236 (1965).
[2]R. L. Farrow and D. W. Chandler, J Chem. Phys. **89**, 1994 (1988).
[3]D. A. V. Kliner and R. N. Zare, J. Chem. Phys. **92**, 2107 (1990).
[4]G. O. Sitz and R. L. Farrow, J. Chem. Phys. **93**, 7883 (1990).
[5]L. M. Hitchcock, G.-S. Kim, E. W. Rothe, and G. P. Reck, Appl. Phys. B **52**, 27 (1991).
[6]D. A. V. Kliner, D. E. Adelman, and R. N. Zare, J. Chem. Phys. **95**, 1648 (1991).
[7]D. Adelman, N. E. Shafer, D. A. V. Kliner, and R. N. Zare, J. Chem. Phys. **97**, 7323 (1992).
[8]K. Mikulecky and K. H. Gericke, Chem. Phys. **173**, 13 (1993).
[9]G. O. Sitz and R. L. Farrow, J. Chem. Phys. **101**, 4682 (1994).
[10]E. de Beer, Y. Zhao, I. Yourshaw, and D. M. Neumark, Chem. Phys. Lett. **244**, 400 (1995).
[11]M. Gostein, H. Parhikhteh, and G. O. Sitz, Phys. Rev. Lett. **75**, 342 (1995).
[12]M. Gostein, E. Watts, and G. O. Sitz, Phys. Rev. Lett. **79**, 2891 (1997).
[13]S. S. Brown, H. L. Berghout, and F. F. Crim, J. Chem. Phys. **107**, 8985 (1997).
[14]A. D. Rudert, J. Martin, H. Zacharias, and J. B. Halpern, Chem. Phys. Lett. **294**, 381 (1998).
[15]J. Han, X. Chen, and B. R. Weiner, Chem. Phys. Lett. **332**, 243 (2000).
[16]S. A. Kandel, A. J. Alexander, Z. H. Kim, R. N. Zare, F. J. Aoiz, L. Bañares, J. F. Castillo, and V. S. Rábanos, J. Chem. Phys. **112**, 670 (2000).
[17]E. Watts, G. O Sitz, D. A. McCormack, G. J. Kroes, R. A. Olsen, J. A. Groeneveld, J. N. P. Van Stralen, E. J. Baerends, and R. C. Mowrey, J. Chem. Phys. **114**, 495 (2001).
[18]E. Watts and G. O. Sitz, J. Chem. Phys. **114**, 4171 (2001).
[19]S. Cureton-Chinn, P. B. Kelly, and M. P. Augustine, J. Chem. Phys. **116**, 4837 (2002).
[20]H. A. Bechtel, J. P. Camden, D. J. A. Brown, and R. N. Zare, J. Chem. Phys. **120**, 5096 (2004).
[21]P. Maroni, D. Papageorgopoulos, A. Ruf, R. D. Beck, and T. R. Rizzo, Rev. Sci. Instrum. **77**, 054103 (2006).
[22]N. C.-M. Bartlett, D. J. Miller, A. J. Alexander, D. Sofikitis, T. P. Rakitzis, and R. N. Zare, Phys. Chem. Chem. Phys. **11**, 142 (2009).
[23]N. C.-M. Bartlett, J. Jankunas, R. N. Zare, and J. A. Harrison, Phys. Chem. Chem. Phys. **12**, 15689 (2010).
[24]N. C.-M. Bartlett, J. Jankunas, and R. N. Zare, J. Chem. Phys. **134**, 234310 (2011).
[25]N. Vitanov, B. Shore, L. Yatsenko, K. Boehmer, T. Halfmann, T. Rickes, and K. Bergmann, Opt. Commun. **199**, 117 (2001);
[26]N. Vitanov, T. Halfmann, B. W. Shore, and L. K. Bergmann, Annu. Rev. Phys. Chem. **52**, 763 (2001).
[27]R. P. Feynman, F. L. Vernon, and R. W. Hellwarth, J. Appl. Phys. **28**, 49 (1957).
[28]N. Mukherjee, J. Opt. Soc. Am. B **23**, 1635 (2006).
[29]N. Mukherjee and R. N. Zare, J. Chem. Phys. **135**, 024201 (2011).
[30]S. Chelkowski and A. D. Bandrauk, J. Raman Spectrosc. **28**, 459 (1997).
[31]L. Allen and J. H. Eberly, *Optical Resonance and Two-Level Atoms* (Wiley, New York, 1975).
[32]R. L. Shoemaker, Annu. Rev. Phys. Chem. **30**, 239 (1979).
[33]D. Grischkowski and M. M. T. Loy, Phys. Rev. A **12**, 1117 (1975).
[34]D. Grischkowski, M. M. T. Loy, and P. F. Liao, Phys. Rev. A **12**, 2514 (1975).
[35]M. M. T. Loy and D. Grischkowski, Opt. Commun. **21**, 379 (1977).
[36]A. S. Pine and G. T. Fraser, J. Chem. Phys. **89**, 6636 (1988).
[37]P. L. Stricklin and D. C. Jacobs, Appl. Opt. **31**, 6983 (1992).
[38]T. T. Kajava, H. M. Lauranto, and R. R. E. Salomaa, Appl. Opt. **31**, 6987 (1992).
[39]T. Rickes, L. P. Yatsenko, S. Steuerwald, T. Halfmann, B. W. Shore, N. V. Vitanov, and K. Bergmann, J. Chem. Phys. **113**, 534 (2000).
[40]L. P. Yatsenko, N. V. Vitanov, B. W. Shore, T. Rickes, and K. Bergmann, Opt. Commun. **204**, 413 (2002).
[41]M. Oberst, H. Muench, G. Grigoryan, and T. Halfmann, Phys. Rev. A **78**, 033409 (2008).